Molecular deformations of halogeno-mesitylenes in the crystal: Structure, methyl group rotational tunneling, and numerical modeling

ARTICLE *in* CHEMICAL PHYSICS · DECEMBER 2002

Impact Factor: 1.65 · DOI: 10.1016/S0301-0104(02)00817-0

5 AUTHORS, INCLUDING:

Marie Plazanet
University Joseph Fourier - Grenoble 1
61 PUBLICATIONS **724** CITATIONS
SEE PROFILE

Jean Meinnel
Université de Rennes 1
61 PUBLICATIONS **256** CITATIONS
SEE PROFILE

Hans Peter Trommsdorff
University Joseph Fourier - Grenoble 1
60 PUBLICATIONS **855** CITATIONS
SEE PROFILE

Available online at www.sciencedirect.com
SCIENCE DIRECT®
Chemical Physics 285 (2002) 299–308
Chemical Physics
www.elsevier.com/locate/chemphys

Molecular deformations of halogeno-mesitylenes in the crystal: structure, methyl group rotational tunneling, and numerical modeling

M. Plazanet[a], M.R. Johnson[d], A. Cousson[b], J. Meinnel[c], H.P. Trommsdorff[a,*]

[a] *Laboratoire de Spectrométrie Physique, Université J. Fourier de Grenoble, CNRS(UMR5588), BP87, St. Martin d'Hères Cedex 38402, France*
[b] *Laboratoire Léon Brilloin, (CEA-CNRS) CEA Saclay, Gif-sur-Yvette Cedex F-91191, France*
[c] *GMCM, Université de Rennes 1, CNRS (UMR6626), Campus de Beaulieu, Bât. 11A, Rennes Cedex 35042, France*
[d] *Institut Laue Langevin, BP156, Grenoble 38042, France*

Received 24 June 2002

Abstract

In crystals of halogeno-mesitylenes, steric hindrance between methyl groups and halogen atoms results in a small out-of-plane deformation of the heavy atoms. Even though these deformations are of very small amplitude, their effect on the rotational potential of the methyl groups is very large because the large threefold contributions to the potential due to the halogens next to a methyl group do not cancel as they do in a planar structure. An investigation of these effects by a combination of computational and experimental methods is presented here for compounds for which precise single crystal structure determinations at low temperatures are available, namely tribromomesitylene and triiodomesitylene, as well as dibromomesitylene for which such a determination was made recently. Information about the rotational potential of the methyl groups is derived from the observed proton densities as well from inelastic and quasi-elastic neutron scattering studies of the tunneling dynamics. DFT calculations reproduce well the molecular structures in the crystal, while a planar structure is predicted for the isolated molecules. The rotational potential of the methyl groups was characterized by DFT and force field calculations at different levels of approximation. The correct calculation of the amplitude of the rotational potential requires the inclusion of the relaxation of all atomic positions during the methyl group rotation, indicating that a one-dimensional model of the rotation is inadequate.

Keywords: Halogeno-mesitylenes; Crystal structure; Steric hindrance; Rotational tunneling

1. Introduction

Force fields, which determine the structure and the dynamics of molecular systems, are established with increasing accuracy by computational methods in combination with experimental data [1]. In

* Corresponding author. Tel.: +33-476-51-47-81; fax: +33-476-63-54-95.
E-mail address: trommsdo@spectro.ujf-grenoble.fr (H.P. Trommsdorff).

0301-0104/02/$ - see front matter
PII: S0301-0104(02)00817-0

particular, the deformation of a molecule in a solid, reflecting the subtle equilibrium between intra- and intermolecular forces, can be used to gauge force fields. Already in an isolated molecule, deformations may arise from the steric hindrance between bulky substituants. The loss of planarity of aromatic molecules in general [2] and of polysubstituted benzene in particular [3] have been classical test cases. Since deformations may be quite small, the precision of structural determinations is often not sufficient, in particular at higher temperatures where thermal motions are important. When the symmetry in the distorted molecule is lowered, indications are, for example, obtained from the mixing of vibrational modes or electronic states making forbidden transitions observable. However the quantitative evaluation of such effects is difficult. In the present work we show how the great sensitivity of tunneling transitions of methyl groups can be exploited to observe small out-of-plane deformations in crystals of halogeno-mesitylenes (1,3,5-halo-2,4,6-trimethylbenzene), and we confront this data with results of numerical studies.

In crystals of halogeno-mesitylenes, the rotation of the methyl groups located between two equivalent halogen atoms is weakly hindered. Isolated trichloro-, tribromo-, and triiodo-mesitylene (TCM, TBM, and TIM) have C_3 symmetry, which is broken in the solid state, resulting in three crystallographically and energetically inequivalent methyl groups. Three different tunneling splittings are thus observed in each compound, ranging from 4 to 13 μeV in TCM, 14 to 49 μeV in TBM, and 14 to 88 μeV in TIM (see Table 1) [4,5]. The crystal structures of these compounds have been accurately determined using single crystal diffraction, down to 120 K for TCM and close to liquid helium temperatures for TBM and TIM [6,7]. Almost free rotation is observed for the methyl group located between the two halogens in dichloromesitylene (DCM) and dibromomesitylene (DBM), interestingly the larger tunneling splitting being observed for DCM (see Table 1) [8].

Table 1
Space group and tunneling splittings of halogeno-mesitylenes

	Crystal structure	Tunneling splittings (μeV)
DBM	$P2_1/n$ (14 K)	392, 0.3, 0.3
DCM	unknown	450
TBM	P (14 K) [6]	25.1, 14.1, 48.8
TIM	$P_{\bar{1}}$ (15 K) [7]	26.7, 14.4, 87.4
TCM	$P_{\bar{1}}$ (~150 K) [11]	4.3, 9.2, 13.1

As in other polysubstituted benzenes, rotations of the entire molecule are observed in these crystals at, or near, room temperature. While these dynamics have motivated numerous studies, they also average structural details. For example, in 1,2,4-trichloro-3,5,6-trimethyl-benzene at 300 K, rotational diffusion by $2\pi/6$ jumps exchanges the position of inequivalent substituants and leads to a disordered, plastic phase at 300 K [9]. Upon cooling, these rotations are quenched and molecular distortions become clearly observable. In the closely related molecule of trichloromesitylene (1,3,5-trichloro-2,4,6-trimethyl-benzene: TCM) the 300 K crystal structure appears ordered by X-ray diffraction measurements, yet the NMR proton T_1 relaxation time indicates that the molecule undergoes rotational diffusion by $2\pi/3$ jumps [10]. TCM undergoes a transition around 150 K into an ordered low temperature phase [11,12].

The issue of if or not the free molecule appears out-of-plane distorted, depends upon the amplitude of vibrations along the direction of the distortion and the time scale of observation. In the crystal field, possible distortions due to the steric hindrance of bulky substituants may be induced or stabilized. The structures of isolated C_6X_6 (X = Cl, Br, I, CH_3) are predicted to be planar and the corresponding crystals to be ordered at any temperature because of the equivalence of the substituants. Measurements made at room temperature suggest that in the crystal, the halogen atoms in C_6Cl_6 [13,14] and C_6I_6 [15] are alternatively arranged above and below the mean plane of the benzene ring at distances of 0.02 and 0.04 Å, respectively. At 130 K, the methyl groups of hexamethylbenzene are located at 0.05 Å from this mean plane [16]. The structure of tetramethylbenzene was determined at 4.2 K, and significantly smaller out-of-plane deviations of 0.01 and 0.017 Å are observed for the two crystallographically inequivalent methyl groups: here in-plane defor-

mations can accommodate part of the repulsive energy [17].

The rotation of methyl groups is hindered by a potential, which has both intra- and intermolecular contributions and the reorientational diffusion of a methyl group is somewhat analogous to the molecular rotational diffusion of substituted benzenes. However, due to the small mass of the molecular rotor, quantum tunneling through the potential barriers dominates at low temperatures, when the diffusive dynamics are quenched, and leads to a splitting of the otherwise degenerate energy levels. This splitting is an exponential function of the height of the barrier hindering the rotation and provides therefore a sensitive probe of the details of the molecular and crystal force field. Provided that the structure is known accurately, the precision of interatomic interactions is gauged, or inversely, using accurate force fields, subtle structural details and more complex dynamical models can be explored. Often a one-dimensional rotational potential, $V(\varphi)$, the Fourier expansion of which can be limited to two terms at most, is sufficiently accurate, so that the Hamiltonian is given by the following expression:

$$H = -B\frac{\partial^2}{\partial\varphi^2} + \frac{1}{2}V_3\cos(3\varphi) + \frac{1}{2}V_6\cos(6(\varphi - \varphi_{36})). \quad (1)$$

The rotational constant of the methyl group is about 650 μeV and represents the limiting value of the tunneling splitting in the absence of a barrier.

While for a simple potential, described by one parameter only, the V_3 or V_6 term is obtained from the measurement of the corresponding tunneling splitting, the evaluation of several parameters of a more complex potential requires additional data, for example the measurement of librational excitations and/or of the change of tunneling splitting upon deuteration of the rotors. When a potential is determined from calculations, the fit of the parameters, V_3, V_6 and φ_{36}, is straightforward. Recently it was shown that in a large number of crystals such one-dimensional rotational potentials, determined by quantum chemistry calculations and in particular periodic density functional theory methods, predict tunneling splittings to within a factor of 2 of the measured values, indicating an error of less than 10% for the barrier heights [18]. In a few cases coupling with other CH_3 groups or with other degrees of freedom must be taken into account.

In this paper, we analyze the methyl group proton density of DBM at 14 and 120 K as obtained in recent single crystal structure determinations [19] and present some additional measurements of the tunneling dynamics of the methyl groups. These results are discussed in the larger context of the available corresponding data for other halogeno-mesitylenes by performing numerical studies of the methyl group rotational potential for this class of compounds. In particular, the following issues are addressed:

Are commonly used methods to establish force fields and rotational potentials sufficient for the prediction of tunneling splittings in these molecules?

Is the origin of the molecular deformations in the solid state intra- or intermolecular?

To what extent does the subtle balance of intra- and intermolecular interactions in the solid state lead to deviations from the simple one-dimensional model of rotation for the methyl groups?

The paper is organized as follows. The new experimental data are presented in the following Section 2. For the molecules for which precise low temperature data are available, DBM, TBM, and TIM, a numerical study of the molecular structures and of the rotational potential is given in Section 3. Finally, in Section 4 we conclude.

2. Crystal structure and tunneling dynamics of DBM

2.1. Crystal structure

Protonated, single crystals of DBM were grown around 0 °C by slowly cooling a saturated solution in dichlorobenzene, so as to avoid a destructive phase transition around 12 °C. The structures at 120 and 14 K were determined by single crystal neutron diffraction and are described in [19]. The 120 and 14 K structures have the same space group, $P2_1/n$. No evidence for a phase transition was found between 120 and 285 K by differential

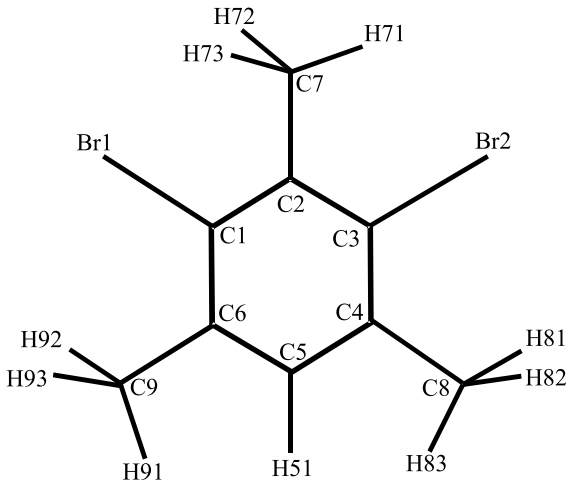

Fig. 1. DBM, numbering of atoms.

scanning calorimetry. The numbering of atoms is given in Fig. 1.

2.2. Proton density

The protons of the methyl group C7 between the two bromine atoms are delocalized at 120 K and become partially localized at 14 K as shown in the Fourier difference maps of Figs. 2(a) and (b), respectively. The Fourier difference maps for the remaining two methyl groups, C8 and C9, show three localized peaks of proton density, indicating significantly more strongly hindered methyl groups. These measured proton densities are confronted below with densities calculated for potentials represented by Eq. (1).

2.3. Tunneling and librational excitations

INS measurements on DBM reveal only one tunneling excitation at 392 μeV [8]. This large tunneling splitting must be assigned to the C7 methyl group, which shows the continuous proton density in the Fourier difference map (Fig. 2). The same INS scan shows two methyl group librational excitations, whose assignment and frequencies were subsequently confirmed in Raman experiments [20]. These two sets of spectroscopic information enabled the refinement of three parameters of the rotational potential given by Eq. (1): $V_3 = 5.28$ meV, $V_6 = 16.72$ meV, $|\varphi_{36}| = 2.5°$ [8].

Tunneling excitations of the more strongly hindered methyl groups, C8 and C9, were initially sought in an INS scan on the backscattering spectrometer IN10 at the ILL [21]. As no peaks could be observed, a so-called fixed window, elastic scan was performed, measuring the elastic intensity at a resolution of 1 μeV as a function of

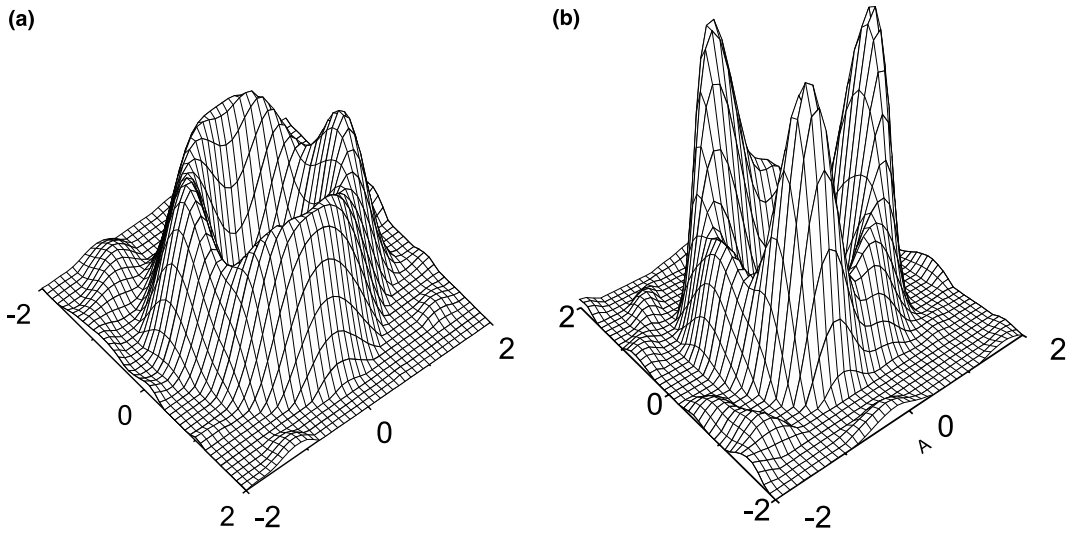

Fig. 2. Fourier difference map in the plane of the C7 methyl protons: (a) at 120 K; (b) at 14 K.

increasing temperature between 10 and 200 K in a scan of 12 h. A monotonic decrease with increasing temperature results from the population of phonons (Debye–Waller effect) while an additional pronounced step over a limited temperature range is observed when the quasi-elastic scattering of the strongly hindered methyl groups becomes broader than the resolution function. The methyl group rotation is here well separated from other molecular motions. This data was analyzed using the so-called thermometer model [22], which relates the thermally activated reorientation rate of methyl groups in a very wide range of solids to the hindering potential, $V(\varphi)$, and the temperature T. This simple theory uses a thermal average, over all methyl group torsion–rotation states, of the modulus of the expectation value of angular momentum.

Fig. 3 shows the experimental data, from which the Debye–Waller decay at low temperature has been removed and the step is rescaled between 0 and 1, superposed with calculated elastic scans predicted for different amplitudes of a simple threefold (V_3 term only) rotational potential. While, in principle, for a given value of momentum transfer, the relative height of the step in the elastic scan can be calculated from the scattering atoms and the number of these involved in thermally activated rotation, this information is complicated by the presence of Bragg peaks. The step in the elastic scan is assigned to the two strongly hindered methyl groups in DBM since both are equivalent in the isolated molecule and their rotational potentials in the solid are expected to be similar, as the Fourier difference maps for both methyl groups are similar. For a pure threefold potential, an amplitude of $V_3 = 75$ meV agrees best with the data. The agreement is improved when an out-of-phase V_6 component is added to the potential with $V_6 = 15$ meV and $\varphi_{36} = 30°$. This increases the distance between librational levels and leads to a steeper slope. The corresponding tunneling splitting is 0.3 μeV, just too small to be measured directly by INS.

2.4. Calculated proton densities

Having determined the potential parameters, proton densities are calculated at different temperatures and confronted with proton densities derived from the Fourier difference maps. This comparison is shown in Figs. 4 and 5 for the weakly and strongly hindered methyl groups, respectively, at 14 and 120 K. For this comparison, the density was integrated over ±0.2 Å along the radius around a value corresponding to the mean distance of the C–H distance in the plane of maximum density.

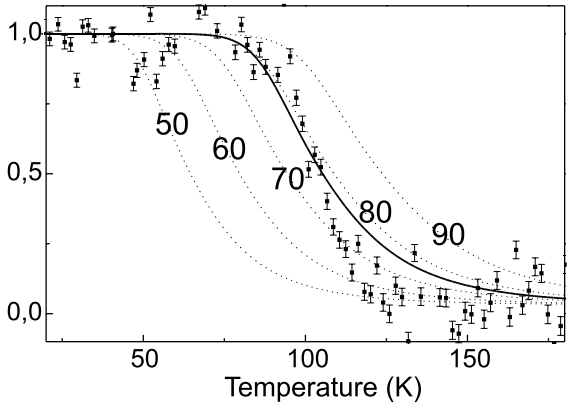

Fig. 3. So-called fixed window, elastic scan. The experimental data are superposed with calculated curves for pure threefold potentials with different amplitudes of $V_3 = 50$–90 meV. The bold curve represents the intensity obtained for the potential: $V_3 = 75$ meV, $V_6 = 15$ meV, and $\varphi_{36} = 30°$.

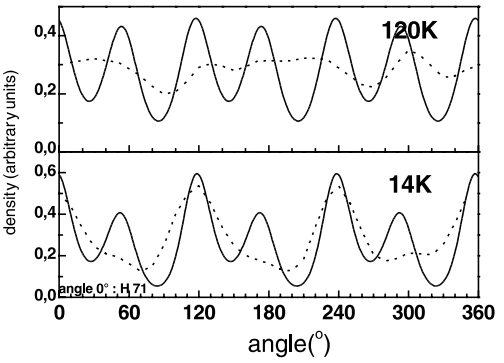

Fig. 4. Comparison of the measured and calculated proton density of the C7 methyl group at 14 and 120 K, as indicated. The three maxima at 0°, 120°, 240° correspond, respectively, to H71, H72, H73.

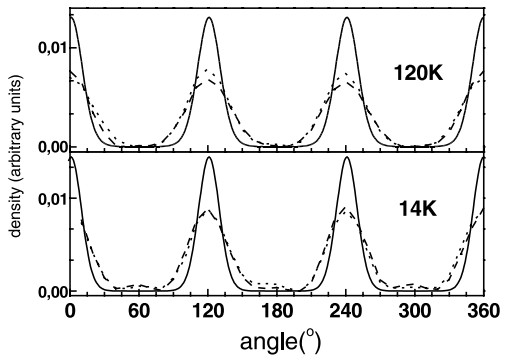

Fig. 5. Comparison of the measured proton density of the C8 (dashed) and C9 (dotted) methyl groups with the average calculated density at 14 and 120 K (solid line) for $V_3 = 75$ meV, $V_6 = 15$ meV, and $\varphi_{36} = 30$.

At both temperatures, the measured proton density of the C7 methyl group is significantly more delocalized than the calculated density. The proton density depends on the sign of the phase, φ_{36}, while the spectroscopic values are insensitive. The measurements clearly indicate a negative sign, thus $\varphi_{36} = -2.5°$. Nevertheless, the fact that the observed proton density is more smeared out indicates that the simple model of one-dimensional rotation may be insufficient for this methyl group.

For the more strongly hindered groups, C8 and C9, the calculated density is again more localized than the measured density and the agreement is only slightly improved by adding a contribution $V_6 = 15$ meV and $\varphi_{36} = 0$. The value of the phase disagrees with the value derived from the fixed-window scan. In the prediction of the proton density, phonon contributions must be taken into account: from a Translation-Libration-Screw analysis of the nine carbon atoms, the broadening of the density due to the rigid rotation and libration of the carbon frame is estimated to be around 7° and this contribution partially explains the disagreement between calculated and predicted widths. Since molecular motions are better separated in the elastic scan, the rotational potential derived from this data is finally retained.

The precision sought in the preceding analysis is justified by the successful confrontation of diffraction and spectroscopic measurements in TBM [6]. In this system, quasi-perfect agreement was found for measured proton densities with densities calculated for rotational potentials (V_3, V_6, φ_{36}) derived from data of tunneling and torsional excitations.

3. Numerical studies of the molecular structure and of the methyl group rotational potential

The accurate structural information available for DBM, TBM, and TIM warrants a detailed numerical study of the origin of the molecular out-of-plane deformations. The observed, absolute mean deviation of the heavy atom substituants from the plane defined by the benzene ring are 0.018 ± 0.001, 0.024 ± 0.001, and 0.045 ± 0.001 Å for DBM, TBM, and TIM respectively (Fig. 6). Expectedly, the out-of-plane deviations of the heavy atoms become larger as the steric hindrance between substituants increases.

3.1. Structures

Investigating the origin of the observed molecular deformations entails determining the stability of the measured structures both in the solid state and for isolated molecules. We have used quantum chemistry methods based on density functional theory (DFT) for solid state and single molecule calculations to estimate the relative importance of inter- and intramolecular interactions. For isolated molecules, we used Gaussian [23] to perform DFT calculations with the B3LYP functional and the 3-21G* basis set, the largest which can be conveniently used for halogens. For the crystal, we employed the periodic DFT code CASTEP, available in the Cerius^2 program [24], which uses plane waves to develop the electron density throughout the simulation cell of a periodic system. Unless otherwise stated, we have used ultrasoft pseudopotentials to describe the nuclei and closed shell electrons, the GGA approximation for the exchange-correlation energy, an energy cut-off of 320 eV for the plane waves and a k-point spacing of 0.01 Å^{-1} for sampling reciprocal space.

The results obtained for isolated molecules are unambiguous, all optimized structures are planar to better than 0.001 Å (except of course the CH_3

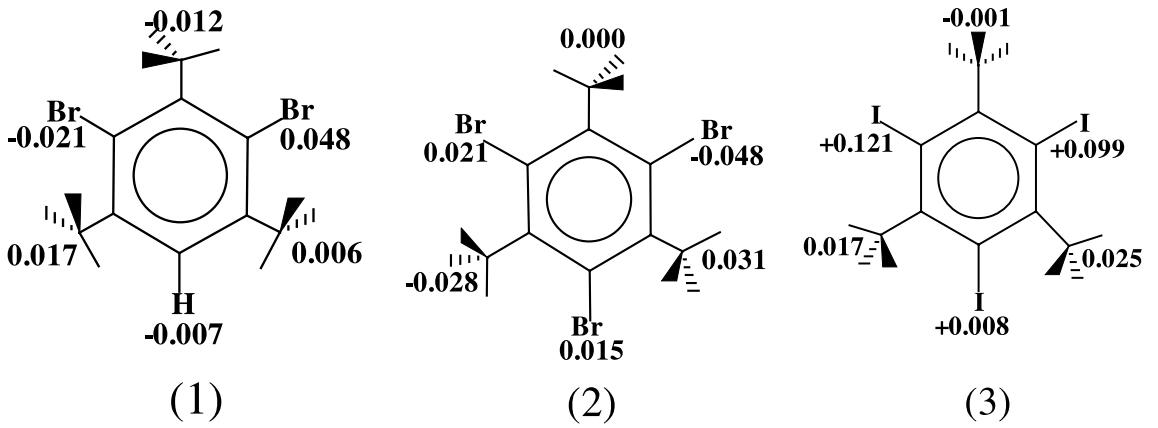

Fig. 6. Deviations of heavy atoms from the best plane through the cycle. The experimentally observed orientations of protons in methyl groups are indicated. (1) DBM, (2) TBM, (3) TIM.

hydrogens). Furthermore, the stability of conformations with various initial orientations of the methyl groups was investigated. As illustrated in Fig. 6, conformations observed in the crystal correspond in general to methyl group orientations with one hydrogen in the plane of the molecule, only for one CH_3 of TIM, the hydrogen lies in a perpendicular plane. For TBM and TIM all conformations converged either to the experimental conformation of TBM, or a conformation with an energy higher by about 5 meV where one CH_3 group points in the opposite direction. An analogous behavior was found for DBM, where only one metastable conformation with an energy of near 100 meV survived.

The stability of the crystal structures was calculated by optimizing the atomic co-ordinates in the measured unit cell. Relaxing the unit cell leads to an unphysical expansion due to the absence of dispersive interactions in the DFT–GGA approximation. Imposing a fixed cell can be equated to an applied external pressure which compensates for the missing interactions. In this way, energetically stable structures are found very close to the observed structures. The calculated, mean absolute deviations of heavy atoms from the benzene plane, in the crystalline phase, are 0.026, 0.028, and 0.057 Å for DBM, TBM, and TIM, respectively, in good agreement with the measured values. For comparison, structures of quasi-isolated molecules were investigated using the same method by considering a single molecule in a cubic cell of $10 \times 10 \times 10$ Å^3. For the calculation of electronic energy, only the Γ point in reciprocal space was used. Out-of-plane deformations were found in this cell even when starting from planar molecular structures. These deformations were found to decrease when taking a larger cell of $12 \times 12 \times 12$ Å^3 and were therefore attributed to residual long-range (Coulomb) interactions. The calculations illustrate the sensitivity of these molecules to external forces regarding possible out-of-plane deformations. We conclude that the out-of-plane deformations in the crystal are induced by intermolecular interactions and find that the methyl group conformations, determined in the crystal, belong to the most stable ones in isolated molecules.

3.2. Methyl group rotational potential

In Section 2, the parameters describing the methyl group rotation in a one-dimensional potential had been derived from experimental data. Here these parameters are deduced from numerical calculations at different levels of approximation, addressing in particular the issue of the importance of out-of-plane deformations during the rotation of the methyl groups. An indication of the contribution of the coordinate along an out-of-plane deformation to the trajectory describing the rotation of the methyl groups is given by the relative weight of the V_3 and V_6 terms to the potential given by

Eq. (1). For a methyl group between two halogens in an isolated, planar, symmetric molecule, only the V_6 term should exist since the V_3 contributions cancel each other. While V_3 terms are restored in a statically out-of-plane distorted molecule, they remain absent if the molecule can fully relax during the rotation. The presence of V_3 terms is thus entirely due to the crystal field.

In most cases studied to this date, calculations of one-dimensional methyl group rotational potentials in a rigid environment successfully reproduce the observed tunneling splittings, provided that the calculated force field is sufficiently precise. In particular, the periodic DFT codes implemented in CASTEP and VASP have been used [1,18]. The possibility to relax other atomic positions during the rigid body rotation of the methyl group is not implemented in these programs, due to the use of Cartesian coordinates, while the required constraints are trivially imposed in single molecule DFT calculations (e.g., Gaussian) that use the z-matrix formalism to describe structures. As single molecule methods do not include the crystal field responsible for the out-of-plane molecular deformations, additional calculations were performed using the empirical force field provided in COMPASS, where the effect of relaxing atomic positions during the rotation could be studied. All calculations were performed for each of the three methyl groups of the three samples investigated.

For the one-dimensional calculation with CASTEP, the relevant methyl group is symmetrized and rotated through 120° in 8 discrete steps of 15°, the electronic structure is calculated for each configuration of nuclei, and the corresponding variation in crystal energy is the one-dimensional rotational potential. The convergence of the calculation was tested as a function of (a) the size of the simulation cell, (b) the number of basis functions used, and (c) the density of the sampling of the electronic wavefunction in reciprocal space. By performing equivalent calculations on increasingly larger simulation cells using computationally faster force field methods, the single unit cell for each system was found to ensure a precision of better than 2% for the rotational potential. A similar le-

Table 2
Comparison for the nine methyl rotors between tunneling splitting (μeV) and potential parameters. V_3 (meV), V_6 (meV), φ_{36} (°), obtained from measurement (a) and calculation (b–f) in the five different approaches. (b) CASTEP: isolated molecule with experimental geometry, (c) CASTEP: crystal with experimental equilibrium geometry, (d) CASTEP: crystal with optimised equilibrium geometry, (e) COMPASS: crystal with optimized equilibrium geometry, (f) COMPASS: crystal with geometry optimized at each step of rotation

Compound	(a)	(b)	(c)	(d)	(e)	(f)
DBM, C7	*392*	*370*	*71*	*3.9*	*15*	*590*
	5.3, 16.7, −2.5	6.0, 3.1, 6.9	17, 2.1, −10.2	38.8, 2.5, 8.5	31.5, 7.6, 3.2	1.9, 2.6, 15.6
DBM, C8	*0.3*	*0.2*	7×10^{-3}	6×10^{-3}	*0.01*	*0.1*
	75, 15, 30	73, 1.6, 0.5	114.6, 3.1, 0.8	116.8, 2.9, 0.9	112.2, 7.1, 0.7	80.2, 5.0, 4.2
DBM, C9	*0.3*	*0.1*	3×10^{-2}	3×10^{-2}	*0.1*	*0.8*
	75, 15, 30	75, 1.8, 1.4	95, 2.8, 0.2	94.2, 2.6, 0.8	79.6, 6.3, 7.8	55.1, 3.0, 9.8
TBM, C7	*25*	*3.6*	*0.8*	*0.1*	*1.2*	*30*
	22.3, 8.7, 31	43.2, 3.4, 1.1	59, 4.8, 0.9	77.9, 7.3, 4.6	45.9, 5.6, 26.3	23.4, 3.3, 9.6
TBM, C8	*14*	*3.9*	*0.3*	*0.1*	*0.2*	*4.4*
	32.0, 8.0, 29	41.7, 3.7, 3.2	67.8, 4.3, 3.4	78.6, 5.8, 7.2	79.8, 13.7, 5.0	36.9, 3.4, 14.9
TBM, C9	*49*	*3.9*	*3.2*	*0.5*	*0.3*	*25*
	25.9, 12.1, 23	42.0, 3.2, 0.2	45.4, 3.6, 4.3	63.9, 5.7, 0.6	71.2, 9.8, 7.5	24.8, 2.1, 1.3
TIM, C7	*27*	*24*	*3.2*	*0.7*	*0.3*	*18*
		23.5, 3.5, 24.2	41, 4.3, 24.5	51.1, 5.8, 28.3	62.0, 12.9, 17.2	24.2, 5.3, 16.3
TIM, C8	*14*	*4.3*	*1.6*	*1.0*	*0.1*	*25*
		42.5, 4.1, 2.5	53.2, 4.4, 0.6	55.6, 5.4, 2.7	87.6, 13.3, 5.6	23.4, 5.1, 11.2
TIM, C9	*87*	*60*	*42.6*	*2.6*	*0.1*	*13*
		19.1, 3.2, 10.9	23.2, 4.0, 1.5	46.4, 5.2, 1.4	83.7, 9.6, 7	24.1, 6.3, 25.9

vel of precision was obtained using the "fine" basis set (energy cut-off 320 eV) and a k-point spacing of 0.01 Å^{-1}. The calculations were made for three situations: (i) experimental atomic positions and cell parameters, (ii) optimized atomic positions with the experimental cell parameters and (iii) the molecule with the experimental geometry of the crystal quasi-isolated in a cell of $10 \times 10 \times 10$ Å^3 (see Section 3.1).

The results of these calculations, regarding the tunneling splitting and the potential parameters are collected in Table 2, together with the experimental data. In contrast to the previous experience with analogous DFT calculations for a large number of different compounds, the agreement between calculation and experiment is mediocre. In order to ascertain the validity of the pseudopotentials used to describe the halogen nuclei and the core electrons, the set of calculations was repeated using another plane-wave DFT code, VASP [25–28]. Comparable results were obtained. In the light of recent work on the effect of coupling between methyl groups [29], coupling potentials were also calculated using force field methods, but these were found to make an insignificant contribution to the SPM potentials. By comparing the results in the different columns, the sensitivity of the potential to the level of approximation is apparent. Comparison of columns (b) and (c) exposes the influence of the environment on the potential, while the change between (c) and (d) exhibits the sensitivity to the precise geometry. The disagreement between DFT and force field calculations is apparent from the comparison of (d) and (e). Note that in both cases the geometry was optimized in identical unit cells. The difference between (e) and (f) demonstrates the large effect of relaxing the geometry during the rotation of the methyl group. The geometry relaxation during the rotation of the methyl group, obtained in the classical force field calculation (f), entails a motion of the whole molecule as well as a deformation of the molecule. Major deformations are in-plane and out-of-plane displacements of the methyl group and halogen atoms, which maximize the separation to the methyl group. The maximum out-of-plane bending amplitude is $<5°$, while in-plane bending remains below 1°. Halogen and methyl groups execute correlated trajectories of maximum radius 0.15 Å. The maximum amplitude of the center-of-mass displacement of the whole molecule is 0.1 Å. The atomic displacements along the tunneling trajectory are of course much smaller.

As already mentioned, this geometry relaxation is not been implemented in the CASTEP code. Assuming that analogous changes result in this case, the calculated and observed tunneling splittings, would agree to within a factor of two or three, a precision customarily obtained in DFT calculations. The ratio of the V_6 over V_3 contribution also increases significantly in agreement with the analysis of the spectroscopic data. It is obvious that these compounds are special in the extreme sensitivity of the methyl group potential to small geometry changes, which must be taken into account in the calculation of the rotational potential energy surface.

4. Conclusion

In halogeno-methyl benzenes, the repulsion between substituants is not quite sufficient to break the planarity of the heavy atom structure in the isolated molecule but makes the molecule very sensitive to external forces in the solid state so that small out-of-plane deformations are observed in the crystal. High-level, periodic DFT quantum chemistry calculations reproduce the energetic stability of the measured out-of-plane deformations. The extreme sensitivity with regard to these deformations is indicated by the periodic DFT calculations when optimizing the geometry of a single molecule isolated in a large box. Even in a cube of $(12\ \text{Å})^3$, Coulomb interactions between neighboring molecules separated by 12 Å lead to significant out-of-plane deformations. In order to eliminate this effect of long-range interactions, true single molecule calculations using Gaussian were required to confirm the planar structure of isolated molecules.

Even though all deformations are of very small amplitude, their effect on the rotational potential is very large since the large threefold contributions to the potential due to the halogens next to a methyl group no longer cancel. Because of this high sen-

sitivity, even a small modulation of these deformations must be taken into account in order to describe correctly the observed rotational tunneling dynamics and proton density distribution of the methyl groups. Multi-dimensional tunneling dynamics are inferred since the one-dimensional model of rotation does not allow a consistent interpretation of the structure and dynamics using proven quantum chemistry based total energy calculations.

An other limitation of the adiabatic relaxation investigated here is that the methyl groups are treated independently, and co-operative rotation driven by the dynamical fluctuations of the halogen positions were neglected. However, neither experimental nor theoretical techniques are currently capable of resolving such complex tunneling dynamics (full geometry optimization and molecular dynamics simulations show correlated classical motions, but do not allow tunneling splittings to be calculated). Only for the most weakly hindered methyl group in DBM, measurements at higher resolution might reveal structure in the tunneling spectrum. Alternatively, NMR studies could reveal these effects [30].

Acknowledgements

We are grateful to N. Fukushima for help with the Gaussian98 calculations, and to D. Mc Grouther for preliminary calculations during a summer placement at ILL.

References

[1] M.R. Johnson, G.J. Kearley, Ann. Rev. Phys. Chem. 51 (2000) 297.
[2] M. Ali Asgar, C.A. Coulson, J. Chem. Soc. (1959) 1558.
[3] C.A. Coulson, D. Stocker, Molec. Phys. 2 (1959) 397.
[4] J. Meinnel, C.J. Carlile, K.S. Knight, J. Godard, Physica B 226 (1996) 238.
[5] J. Meinnel et al., Physica B 180 & 181 (1992) 711.
[6] J. Meinnel, M. Mani, A. Cousson, F. Boudjada, W. Paulus, M.R. Johnson, Chem. Phys. 261 (2000) 165.
[7] A. Boudjada, J. Meinnel, A. Boucekkine, O. Hernandez, M.T. Hernandez-Diaz, J. Chem. Phys., in press.
[8] J. Meinnel, B. Hennion, M. Mani, B. Wyncke, C.J. Carlile, Physica B 213 & 214 (1995) 649.
[9] G.-P. Charbonneau, J. Trotter, J. Chem. Soc. A (1967) 2032.
[10] M. Eveno, J. Meinnel, J. Chim. Phys. 63 (1966) 108.
[11] T. Fujiwara, T. Atake, H. Chihara, Bull. Chem. Soc. Jpn. 63 (1990) 657.
[12] M. Tazi, J. Meinnel, M. Sanquer, M. Nusimovici, F. Tonnard, R. Carrie, Acta Cryst. B 51 (1995) 838.
[13] G.M. Brown, O.A.W. Strydom, Acta Cryst. B 30 (1974) 801.
[14] A.M. Levelut, M. Lambert, Mol. Cryst. Liquid Cryst. 23 (1973) 111.
[15] R.J. Steer, S.F. Watkins, P. Woodward, J. Chem. Soc. C (1970) 403.
[16] W.C. Hamilton, J.X. Edmonds, A. Topper, J.J. Rush, Discuss. Faraday Soc. 48 (1969) 192.
[17] M. Plazanet, M.R. Johnson, J.D. Gale, T. Yildirim, G.J. Kearley, M.T. Fernández-Díaz, D. Sánchez-Portal, E. Artacho, J.M. Soler, P. Ordejón, A. Garcia, H.P. Trommsdorff, Chem. Phys. 261 (2000) 189.
[18] M.N. Neumann, PhD Thesis, Grenoble, France (1999).
[19] M. Plazanet, A. Cousson, J. Meinnel, M. Nierlich, Acta Cryst., submitted.
[20] M. Plazanet, M.N. Neumann, H.P. Trommsdorff, Chem. Phys. Lett. 320 (2000) 651.
[21] http://www.ill.fr/YellowBook/IN10/.
[22] S. Clough, A. Heidemann, A.J. Horsewill, J.D. Lewis, M.N.J. Paley, J. Phys. C: Solid State Phys. 15 (1982) 2495.
[23] Gaussian 98, User's reference guide, Gaussian Inc., Carnegie Office Park, BLDG. 6; Pittsburg, PA 15106 USA.
[24] Cerius2 User's manual, Molecular Simulations Inc., 9685 Scranton Road, San Diego, CA 92121-3752, USA.
[25] G. Kresse, J. Hafner, Phys Rev. B 47 (1993) 558.
[26] G. Kresse, Thesis, Technische Universität Wien (1993).
[27] G. Kresse, J. Furthmüller, Comput. Mat. Sci. 6 (1996) 15.
[28] G. Kresse, J. Furthmüller, Phys. Rev. B 54 (1996) 11169.
[29] M.A. Neumann, M.R. Johnson, P.G. Radealli, H.P. Trommsdorff, S.F. Parker, J. Chem. Phys. 110 (1999) 516.
[30] C. Choi, M.M. Pintar, J. Chem. Phys. 106 (1997) 3473.